International Journal of Materials and Chemistry 2014, 4(2): 15-26
DOI: 10.5923/j.ijmc.20140402.01

Influence of Amount of Silver on the Structural and Optical Properties of TiO_2 Powder Obtained by Sol-Gel Method

Agnieszka Hreniak, Andrzej Sikora, Agnieszka Iwan*

Electrotechnical Institute, Division of Electrotechnology and Materials Science, M. Sklodowskiej-Curie 55/61 Street, 50-369 Wroclaw, Poland

Abstract In this paper five TiO_2 powders prepared by sol-gel technique were analyzed being into consideration the modification of method of synthesis applied. As a precursors titanium (IV) buthoxide (TBOT) or titanium (IV) isopropoxide (TIPO) were used. The size of obtained pure TiO_2 particles (called in paper TiO_2-1 ÷ TiO_2-5) was in the range 80-300 nm as it was confirmed by XRD, SEM and AFM techniques. Ag doped TiO_2 (abbreviated herein as TiO_2-2-Ag-y) was obtained using two methods of synthesis, where different amount of silver was added (1, 5 or 10% w/w). Additionally, the influence of method of the synthesis applied and amount of silver on the UV-vis properties of TiO_2 was analyzed.

Keywords TiO_2, Nanoparticles, Ag doped TiO_2

1. Introduction

Titanium dioxide (TiO_2), an example of metal-oxide type semiconductors, has been broadly studied and widely used in different applications such as a photocatalytic material for self-cleaning coatings, environmental purifiers, antifogging mirrors and many others [1, 2]. Being into consideration practical application of TiO_2, a lot of work is also dedicated obtained titania with different ions [1, 3-9]. As the sub-micrometer size TiO_2 powders are promising materials, further investigations are desired, with the tools providing reliable and complex high-resolution information about observed objects. Therefore, atomic force microscopy (AFM) along with scanning electron microscopy (SEM) [10-12] and transmission electron microscopy (TEM) [13-15] becomes an important diagnostic instrument allowing obtain the information about electrical, magnetic and thermal properties of such a small objects [16-19]. It should be underlined, that due to wide range of measurement conditions such as: temperature, environment, magnetic field in connection to very simple preparation procedure [20-21] AFM has become very popular among researches worldwide. As it provides quantitative topography information, one can extract the particle size data, however the influence of the shape of the scanning tip should be taken into account [22, 23]. Moreover, the shape of the grains may be a source of useful information. Additionally, direct tip-sample contact in both: contact and intermittent contact modes as well as various derived techniques, may be used in determination and mapping of the mechanical properties of investigated material [24-26].

The main goal of this work was investigation influence of amount of silver on the structural and optical properties of TiO_2 powder via XRD, SEM, AFM and UV-vis methods. A special emphasize was put to investigated obtained titania powders via AFM technique.

* Corresponding author:
a.iwan@iel.wroc.pl (Agnieszka Iwan)
Published online at http://journal.sapub.org/ijmc
Copyright © 2014 Scientific & Academic Publishing. All Rights Reserved

2. Materials and Methods

2.1. Materials

Titanium(IV) buthoxide (TBOT) (99+%) and titanium(IV) isopropoxide (TIPO) (99+%) were purchased from Alfa Aesar. Ethanol (96%), isopropyl alcohol, silver nitrate $AgNO_3$ was purchased from POCh Gliwice.

2.2. TiO_2 Powder Synthesis

TiO_2 powders were prepared by sol-gel method using as titanium precursor titanium(IV) buthoxide (TBOT) or titanium(IV) isopropoxide (TIPO). Titanium precursor was dissolved in ethanol (or isopropyl alcohol) mixed with 3.5 ml of distilled water yielding a titania sol. The solution was stirred in a plastic flask at room temperature for 4 h. During the stirring the titania powder was formed and after filtering was dried at room temperature. The TiO_2 powder was heated at 500°C for one hour. Details about synthesis of TiO_2 are presented in Table 1.

Table 1. Details about synthesis of TiO_2

Code	Details about synthesis
TiO_2-1	4.5 ml of TBOT, 21 ml of ethanol, 3.5 ml of distilled water
TiO_2-2	4.5 ml of TIPO, 21 ml of ethanol, 3.5 ml of distilled water
TiO_2-3	4.5 ml of TIPO, 42 ml of ethanol, 3.5 ml of distilled water
TiO_2-4	4.5 ml of TIPO, 10 ml of isopropyl alcohol, 3.5 ml of distilled water
TiO_2-5	4.5 ml of TIPO, 10 ml of ethanol, 3.5 ml of distilled water

2.3. Ag Doped TiO_2 Powder

Titania doped with silver were obtained by using two methods of synthesis: TiO_2-Ag-y and TiO_2-Ag-ya. In both cases such components as TIPO, ethanol, and distilled water were applied and stirred during 4 hours. Differences in both methods of synthesis were in the time and order to added $AgNO_3$ to the mixture. To obtain TiO_2-Ag-y $AgNO_3$ was stirred four hours along with other components, while in the case of TiO_2-Ag-ya $AgNO_3$ was added to sol mixture and stirred only 2 hours. Details of the titania-silver synthesis are presented below.

TiO_2-2-Ag-y: TiO_2-2-Ag powder was prepared by sol-gel method using as titanium precursor titanium(IV) isopropoxide (TIPO). Titanium precursor was dissolved in ethanol. Briefly, 4.5 ml of TIPO and 21 ml of ethanol were mixed with 3.5 ml of distilled water and addition of silver nitrate $AgNO_3$ to the obtaining sol with the molar ratio Ag/TIPO equal 1%, 5%, 10% (abbreviated herein as TiO_2-2-Ag-1, TiO_2-2-Ag-5, TiO_2-2-Ag-10). The solution was stirred in a plastic flask at room temperature for 4 h. During the stirring the titania powder was formed and after filtering was dried at room temperature. The TiO_2-2-Ag powder was heated at 500°C for one hour.

TiO_2-2-Ag-ya: TiO_2: Ag-ya powder was prepared by sol-gel method using as titanium precursor titanium(IV) isopropoxide (TIPO). Titanium precursor was dissolved in ethanol. Briefly, 4.5 ml of TIPO and 21 ml of ethanol were mixed with 3.5 ml of distilled water yielding a titania sol. The solution was stirred in a plastic flask at room temperature for 2 h. Next addition of silver nitrate $AgNO_3$ to the obtaining sol with the molar ratio Ag/TIPO equal 1%, 5%, 10% (abbreviated herein as TiO_2-2-Ag-1a, TiO_2-2-Ag-5a, TiO_2-2-Ag-10a) and mixed for 2h. During the stirring the titania powder was formed and after filtering was dried at room temperature. The TiO_2 -2-Ag- ya powder was heated at 500°C for one hour.

2.4. Preparation TiO_2 Samples on the Glass Substrate

In order to perform the AFM measurements of the TiO_2 powders, the microscope glass was used as the substrate. The surface of the glass was covered with cyanoacrylate glue and left for few second for preliminary cure. A small quantity of the powder was carefully placed on the surface of the substrate and left for few minutes to cure the glue. Afterwards, the weakly attached grains of the powder were removed using pressured air, in order to avoid them to stick to the scanning tip. Such an approach allows obtain small agglomerates and single grains on the surface.

2.5. Methods

X-ray diffraction patterns were recorded using powder on a Pulveraceous diffractometer Dron – 2. Co radiation filtrated by Fe was applied. Scanning electron microscopy (SEM) studies were performed with a tungsten cathode Vega II SBH (TESCAN) to examine the morphology of the TiO_2. UV-vis spectra were recorded as films from chloroform solution casted on the glass substrate by using Jasco V670 spectrophotometer. Atomic force microscopy (AFM) measurements were performed with Innova system from Bruker (formerly Veeco) in air, at temperature 23℃ and humidity 35% RH. Two modes were used: intermittent contact (IC-AFM) with phase imaging (PI) feature and force modulation mode (FMM). Both modes deliver morphological information about the surface of the sample. The phase feature imaging allows create a map of the tip-sample energy dissipation as the distance between them changes periodically. The energy dissipation is a complex response and may contain various components related to the surface stiffness, adhesion, presence of electrostatic field and others [27-31]. In order to provide more reliable information source, the force modulation mode derived from contact technique was used. It allows create the stiffness map of the surface [32,33]. The intermittent contact mode measurements were performed using standard MPP-11120 probes from Bruker (k=40 n/m, f_{res}=300 kHz, r_{tip}=8 nm), FMM mode measurements on the other hand were performed using MPP-31100 probes from Bruker (k=0.9 N/m, f_{res}=20 kHz, r_{tip}=8 nm). The scanning speed in both modes was applied at the level 0.2 Hz, providing good surface tracking with minimized risk of the particles attachment to the tip. The data was processed with SPIP software from Image Metrology. In order to provide better readability of the topography images, the Sobel transform data was additionally presented, as it reveals presence of fine structures and was successfully utilized in other papers [34-36].

Zeta potentials of nanoparticles were determined using analyzer Zetasizer Nano ZS Malvern Instruments. In 20 ml H_2O 0.01 g TiO_2 was put. The pH of suspensions was adjusted using 0.1 M HCl or 0.1 M NaOH.

3. Results and Discussion

3.1. Characteristic of TiO_2

3.1.1. X-ray diffraction, SEM and UV-vis

X-ray diffraction and scanning electron microscopy (SEM) were used to analyze the titania. The X-ray spectra of the both TiO_2 powders (TiO_2-1 ÷ TiO_2-5) annealed at 500°C shows the same diffraction pattern characteristic to anatase crystalline phase (see Fig. 1a). A major peak corresponding to (101) reflections of the anatase phase of TiO_2 was apparent at the angle of 29.45°. Our X-ray results are in good agreement with other works dedicated TiO_2 [e.g. 37].

Moreover, for the titania powders TiO_2-3 ÷ TiO_2-5 traces of rutile crystalline phase was found at the angle of 32.00° (see Fig. 1b).

Pure TiO_2-1 ÷ TiO_2-5 powders were investigated by SEM technique. Morphologies of TiO_2-1 and TiO_2-2, as an examples revealed by SEM micrographs are shown in Fig. 2. TiO_2-1 ÷ TiO_2-5 samples appeared as agglomerations of smaller particles. The TiO_2 powder in all cases presented aggregates consisting of smaller particles (from 80 nm for TiO_2-4, to 200 nm for TiO_2-1) to larger particles (from 100 nm for TiO_2-4, to ~300 nm for TiO_2-1).

The grains size shape depends on the synthetic conditions and precursors used. The smallest grain sizes were observed for the reactions with TIPO. The important parameter controlling the particle formation and aggregation was the water/precursor molar ratio (see Experimental part).

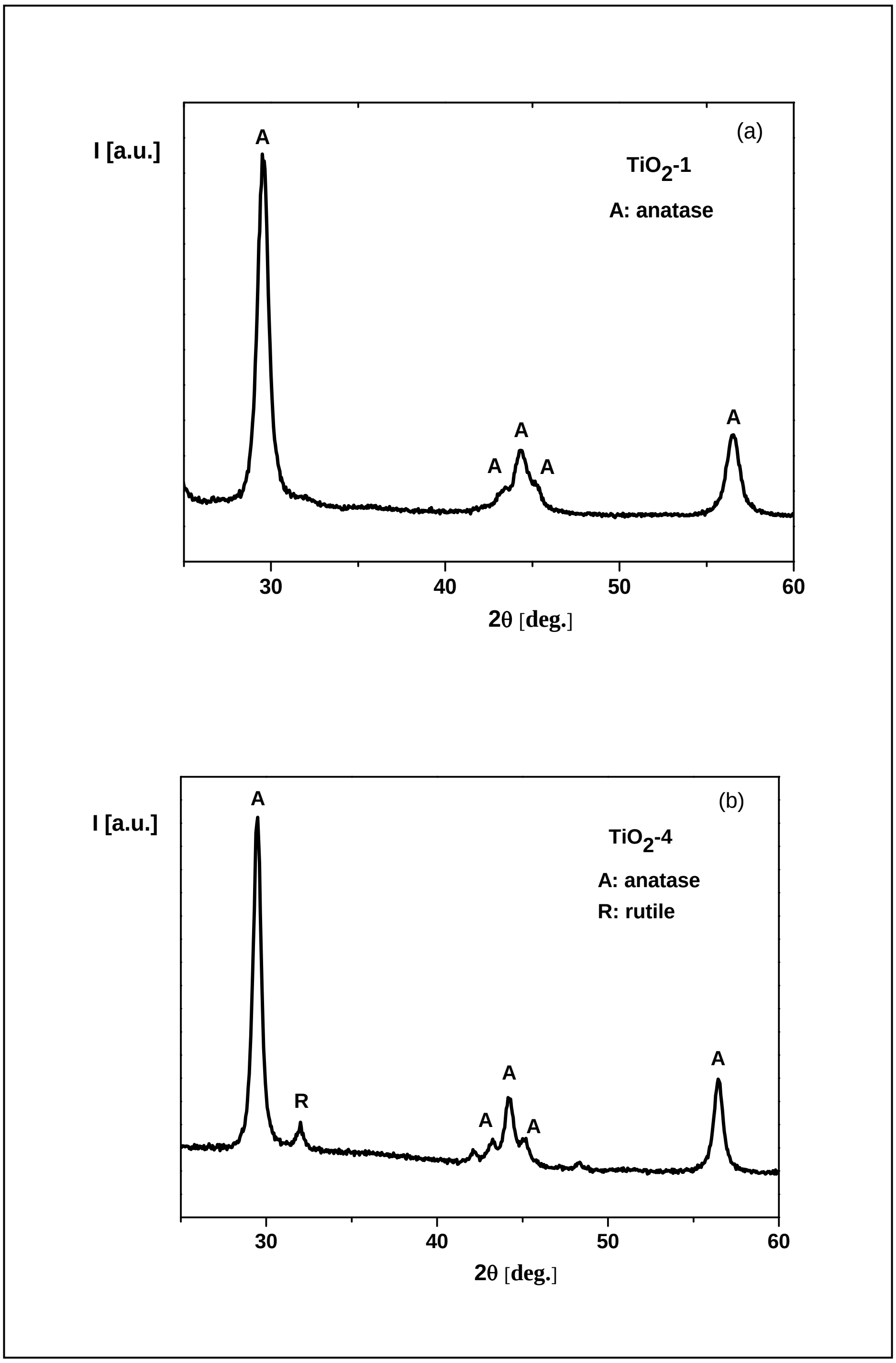

Figure 1. X-ray pattern of TiO_2-1 powder annealed at 500 °C (a), TiO_2-4 powder annealed at 500 °C (b)

The average grain size of obtain pure TiO_2-1 was found about 240 nm, for TiO_2-2 was 170 nm, for TiO_2-3 was 110 nm, for TiO_2-4 was 90 nm while for TiO_2-5 was 160 nm.

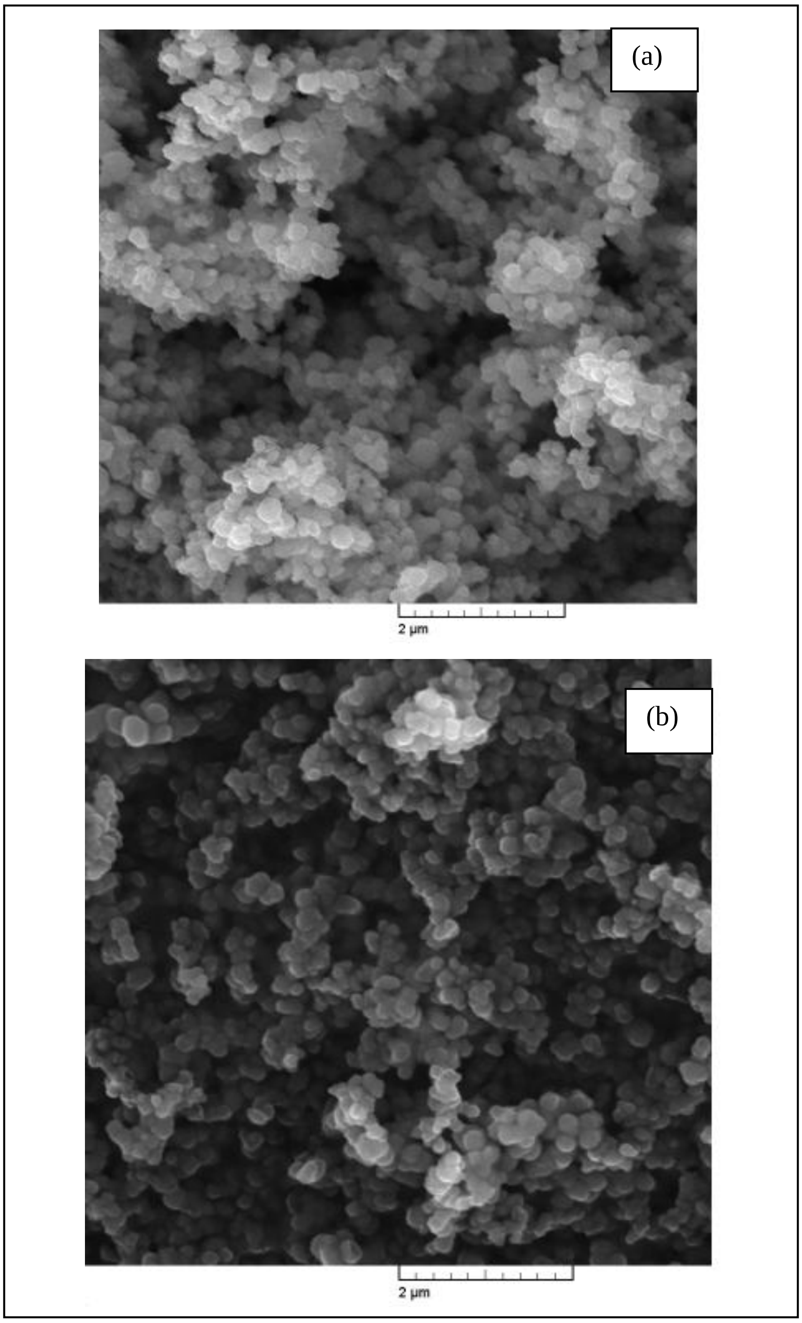

Figure 2. SEM micrographs of titania powders: (a): TiO_2-1 and (b) TiO_2-2

Fig. 3a shows the diffuse reflective UV–vis spectra of pure TiO_2-1 ÷ TiO_2-5 samples. The all TiO_2 samples had strong absorption only in the UV region corresponding to its band gap energy. The obtained results are connected with the value of optical energy gap of investigated samples and are in good agreement with the results described in [37-39].
In order to investigate the visible-light absorption in detail, the Kubelka–Munk functions of all TiO_2-1 ÷ TiO_2-5 samples were calculated. The obtained results are shown in Fig. 3b.

All investigated samples exhibited one absorption maximum band in the range 305-330 nm, depend on the method of synthesis applied to obtained TiO_2 powder. Samples TiO_2-1 and TiO_2-2 were red shifted in comparison with other investigated compounds and exhibited λ_{max} at 330 nm. Samples TiO_2-3 and TiO_2-5 has λ_{max} at about 320 nm while TiO_2-4 was blue shifted in comparison with other compounds (λ_{max} at 305 nm). The values of maximum of UV-vis absorption band detected from the Kubelka–Munk function are presented in Table 2.

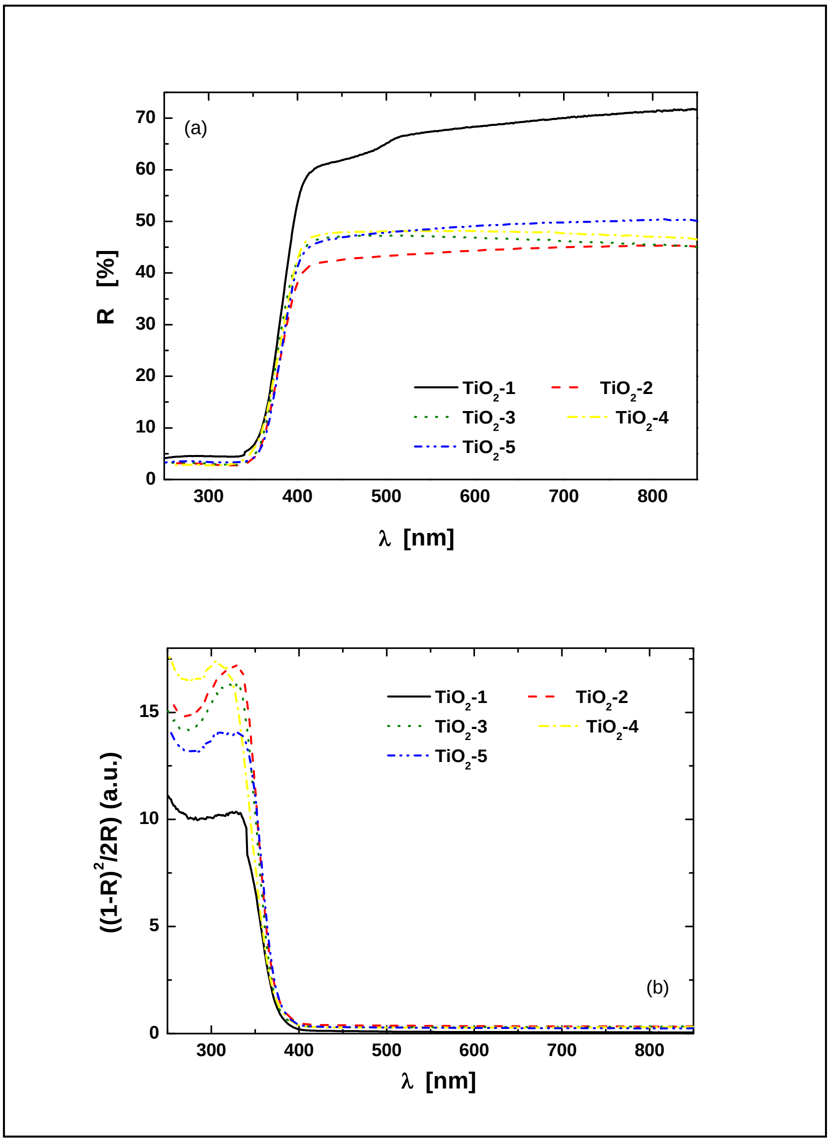

Figure 3. Diffuse reflective UV–vis spectra of TiO_2-1 ÷ TiO_2-5 (a) and Kubelka–Munk function at different wavelengths of TiO_2-1 ÷ TiO_2-5 (b)

Table 2. Absorption UV-vis properties of pure and doped with Ag TiO_2 powder detected from the Kubelka–Munk function

Code	λ [nm]
TiO_2-1	329
TiO_2-2	330
TiO_2-3	323
TiO_2-4	305
TiO_2-5	320
TiO_2-2-Ag-1	326
TiO_2-2-Ag-1a	328
TiO_2-2-Ag-5	576, 332
TiO_2-2-Ag-5a	566, 323
TiO_2-2-Ag-10	622, 332
TiO_2-2-Ag-10a	609, 332

3.1.2. AFM Study

The AFM measurements of the TiO_2 samples were performed in intermittent contact mode. Several measurements have been taken in order to provide statistically significant data. As the powder easily agglomerates, the optical camera view was used to place the scanning tip in areas covered with smallest visible objects, allowing to assume, that desired quality data will be collected with minimum risk of the tip contamination. Obtained result allowed to determine the diameter of the grains by analyzing the profile of the surface. The readouts were done in case of grains with clearly imaged both opposite edges. It should be underlined, that the impact of the shape of the scanning tip could be neglected in case of observed structures. The data obtained with AFM and SEM are consistent. The grains have regular, round and smooth shape. The example of acquired topography with its Sobel transform for TiO_2-2 is presented in Fig. 4.

In our work we investigated the influence of two titanium precursors on the structural and optical properties of synthesized TiO_2. As precursors we used TBOT (TiO_2-1) or TIPO (TiO_2-2). For details of synthesis see Table 1. Being into consideration kind of precursor used, we can conclude that the average grain size was smaller for the titania obtained from TIPO (TiO_2-2) than from TBOT. On the other hand, kind of precursor applied to obtain TiO_2 not influence on the absorption UV-vis properties and kind of crystalline phase of titania (see Table 2).

Moreover, we investigated influence of kind and amount of the solvent on the structural and optical properties of the synthesized titania. As a solvent we used ethanol or isopropyl alcohol (see Table 1). Being into consideration kind of the alcohol applied we can conclude that the average grain size was smaller for the titania obtained from isopropyl alcohol (TiO_2-4) than from ethanol (TiO_2-5). It is interesting that we observed big differences in the absorption UV-vis properties of these two materials. Along with change isopropyl alcohol (TiO_2-4) into ethanol 15 nm red shift was found in absorption UV-vis properties of TiO_2 (see Table 2). We not observed changes in the crystalline form of titania along with change isopropyl alcohol (TiO_2-4) to ethanol (TiO_2-5).

Additionally, we investigated influence of amount of ethanol (10, 21 and 42 ml) on the structural and optical properties of titania. Along with increase the amount of ethanol decrease of average grain size was found, clearly seen for the compounds TiO_2-2 (21 ml of C_2H_5OH) and TiO_2-3 (42 ml of C_2H_5OH). No big differences in absorption UV-vis properties were observed for these compounds, however along with increase the amount of ethanol from 10 ml (TiO_2-5) to 21 ml (TiO_2-2) 10 nm red shift was found (see Table 2). Moreover, along with increase the amount of ethanol from 10 ml (TiO_2-5) to 21 ml (TiO_2-2) crystalline phases of titania change from anatase and rutyl to pure anatase form.

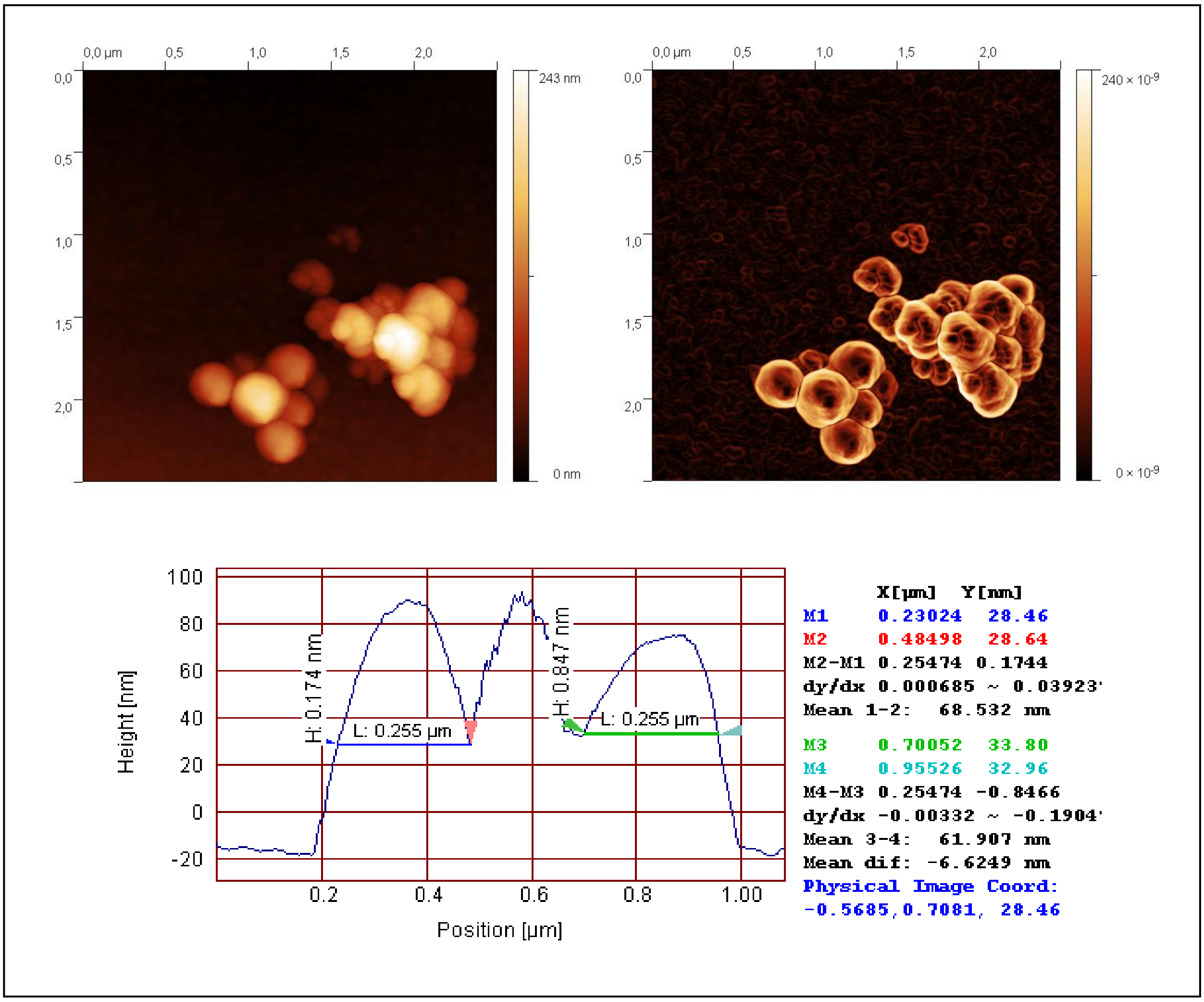

Figure 4. AFM topography of TiO_2-2 (left) Sobel transform of the topography (right), and the profile with markers used for determination of the grain radius

3.2. Characteristic of Ag Doped TiO_2

3.2.1. X-ray Diffraction and EDS and UV-vis

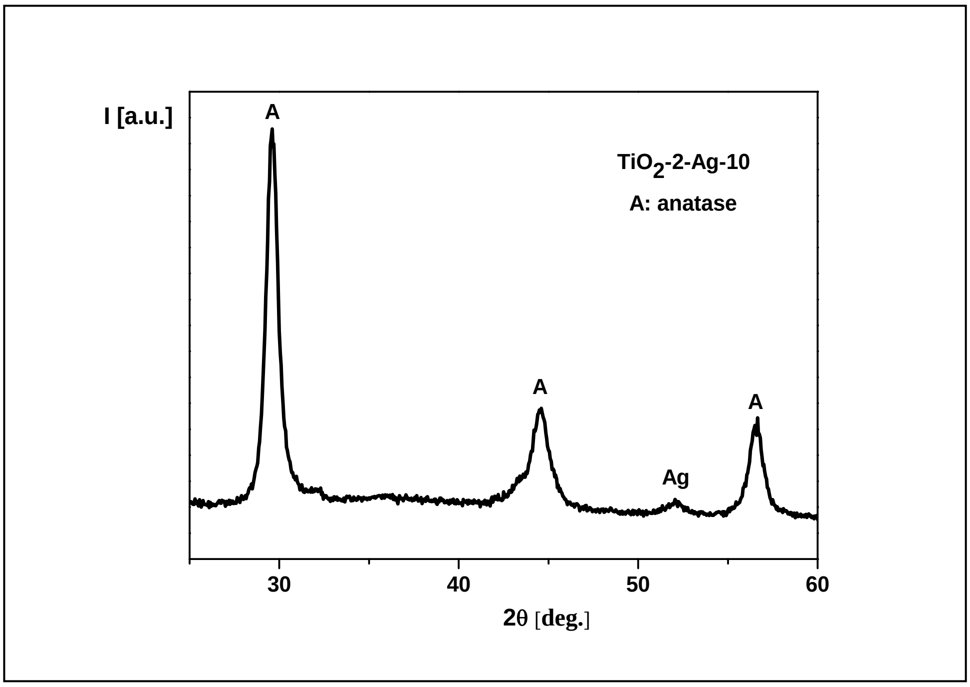

Figure 5. X-ray pattern of TiO_2-2-Ag-10, as an example

For the silver doped titania, X-ray diffraction and scanning electron microscopy (SEM) along with EDS were used. The size of crystallite (D) of Ag doped TiO_2, as was detected by X-ray, was about 130 Ǻ. For all the samples independ on the amount of Ag the same diffraction pattern characteristic to anatase crystalline phase was detected. A major peak corresponding to (101) reflections of the anatase phase of Ag doped TiO_2 was apparent at the angle 29.47-29.75° depend on the method of synthesis used and amount of silver in titania. Small diffraction peak at the angle 52.08° coming from Ag in TiO_2 was only observed in the case of samples with 10% w/w of Ag in titania (see Fig. 5). Moreover, higher amount of Ag in titania was detected by X-ray in the sample TiO_2-2-Ag-10 in comparison with the sample TiO_2-2-Ag-10a. The size of crystallite (D) of Ag in TiO_2, as was detected by X-ray, was about 145 and 128 Ǻ, respectively for TiO_2-2-Ag-10 and TiO_2-2-Ag-10a powders.

Moreover, the amount of Ag in titania was detected with EDS, and is good agreement with our experimental methods. The obtained results are schematically presented in Fig. 6.

Similarly as for pure powders, we analyzed Ag doped titania by UV-vis method. Fig. 7a shows the diffuse reflectance UV–vis spectra of TiO_2-2-Ag-y and TiO_2-2-Ag-ya samples. The all Ag doped TiO_2 samples had strong absorption in the UV region similar as pure powders. Moreover, weak absorption was observed in the range 450 – 800 nm and is caused the presence of Ag in titania. For the silver doped TiO_2, also the Kubelka–Munk functions were calculated. The obtained results are shown in Fig. 7b.

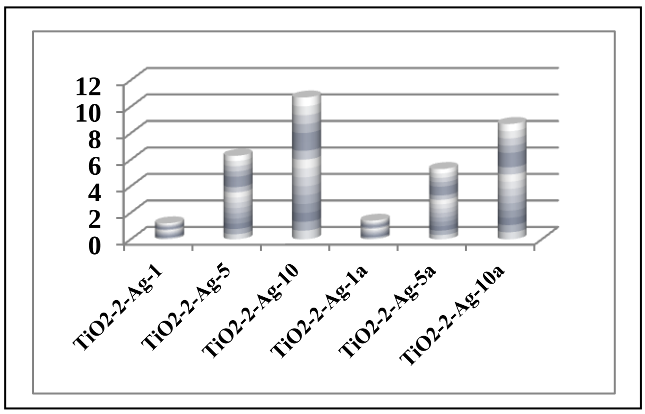

Figure 6. Ag weight content analysis performed with EDS

All investigated Ag doped titania samples exhibited one absorption maximum band in the range of 323-332 nm, depend on the method of synthesis applied to obtained Ag doped TiO_2 powder and amount of Ag in sample. Moreover, along with increase the amount of Ag in titania, second absorption band was observed in the range 566-622 nm (see Table 2). Additionally, increase of amount of silver in titania from 5 to 10% w/w caused increase the absorption intensity of this band. Samples with 10% w/w of Ag in TiO_2-2 exhibited big red shifted in comparison with other investigated compounds (see Table 2).

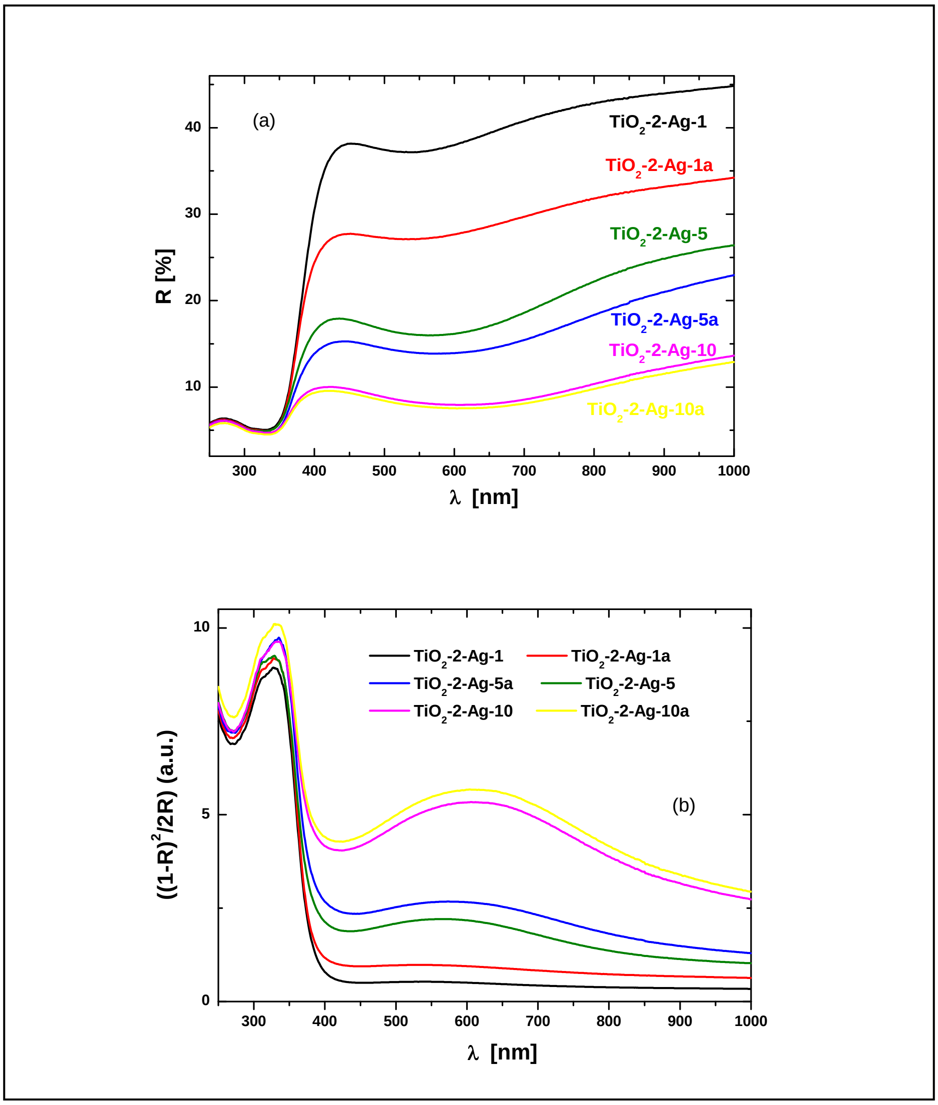

Figure 7. Diffuse reflective UV–vis spectra of TiO_2-2-Ag-y and TiO_2-2-Ag-ya (a) and Kubelka–Munk function at different wavelengths of doped with Ag titania (b)

3.2.2. AFM study

The samples were measured with intermittent contact mode and additionally available phase imaging feature. The example of TiO_2-2-Ag-1AFM image is presented in Fig. 8.

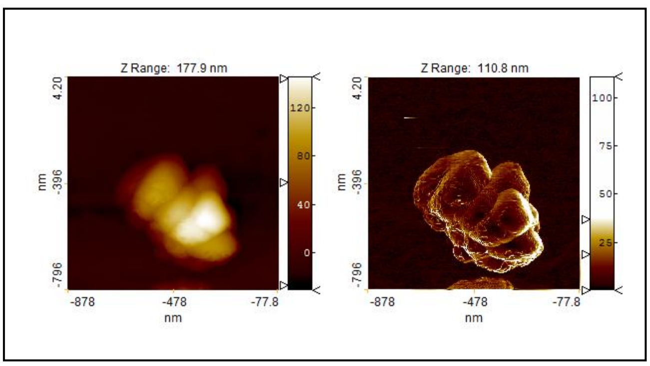

Figure 8. The topography (left) and Sobel transform of the topography of measured TiO_2-2-Ag-1 sample

The topographical information allowed determining the grains diameter. The measurements results are presented in Table 3.

The average diameter of Ag doped TiO_2-2 grains detected with AFM was found about in the range of 30- 200 nm, depend on the amount of silver applied (see Table 3).

Table 3. The averaged diameter values of the Ag doped TiO_2-2 and powder measured with AFM

Code	Average diameter [nm]
TiO_2-2-Ag-1	194
TiO_2-2-Ag-1a	53
TiO_2-2-Ag-5	39
TiO_2-2-Ag-5a	62
TiO_2-2-Ag-10	80
TiO_2-2-Ag-10a	33

As the silver presence could be detected on the surface of the grains as it causes different level of the energy dissipation between oscillating tip and sample, the relevant data was acquired. The phase imaging feature allowed to create additional map, which combined with topography showed the placement of the Ag on the silver. Figure 9 shows 3D view of the topography with color representation of phase imaging response for TiO_2-2-Ag-1, as an example. One can see clearly the areas of two different fractions confirming presence of two materials on the surface.

It should be mentioned, that the interpretation of such a data should be performed carefully, as the PI response can also vary due to tip-sample distance changes caused by limited time response of the microscope (edges or tilted surfaces) as well as the changing contact area between the tip and sample, as scanned objects can have complex shapes and in some spots observed effect may be misleading. In presented data however, such a issues could be easily identified and excluded. Obtained data allowed observing the presence of Ag on the grains surface, allowing this material to be chemically active.

Additionally, the shape of single grains may allow confirm the kind of the material once detected with other method (XRD). Presented images (Fig. 10) illustrate the observation of presence of specific angles and surfaces of the grains, confirming the anatase form of TiO_2-2-Ag-1. The profiles reveal clearly repeatable structure form, with certain angles even though the grains are randomly oriented.

As mentioned before, also the mechanical properties of the sample may be mapped as the direct tip-sample contact allows measuring the interaction force.

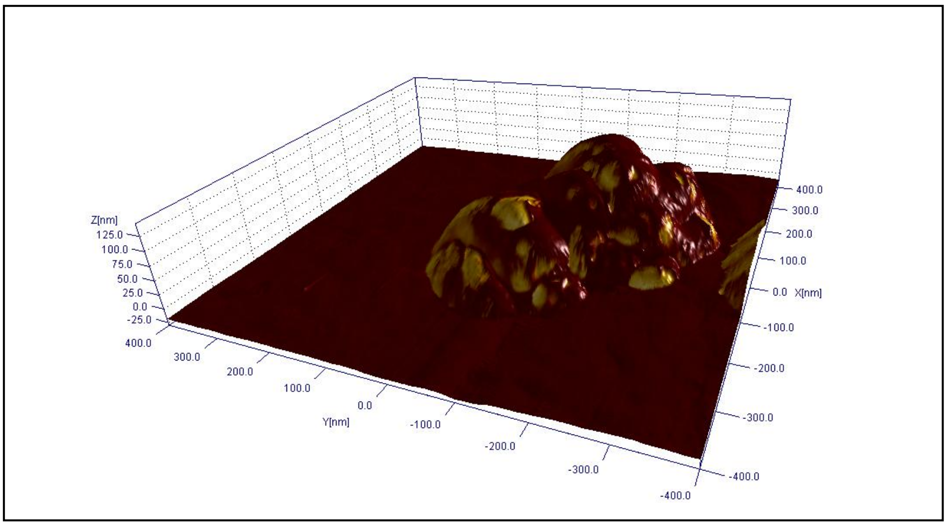

Figure 9. The 3D topography image of the TiO_2-2-Ag-1 with phase imaging data presented with the colors

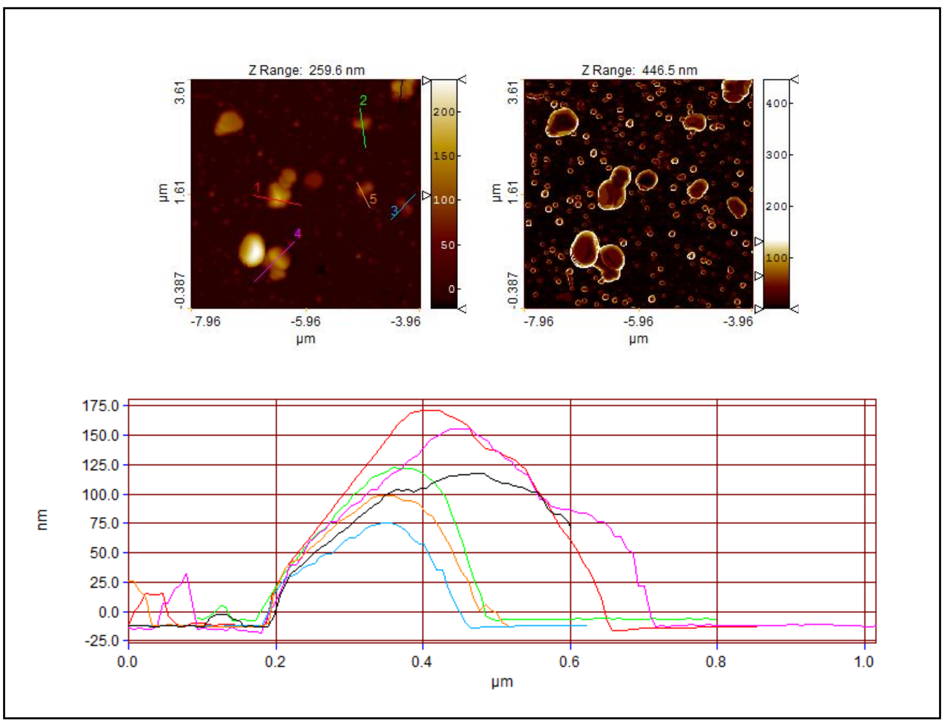

Figure 10. Topography (left) and Sobel transform of the topography (right) as well as the profiles of investigated TiO_2-2-Ag-1 sample

Utilization of force modulation mode enables recognition of soft and hard areas of investigated surface. The results of the measurements of the TiO_2-2-Ag-1 sample are shown in Fig. 11.

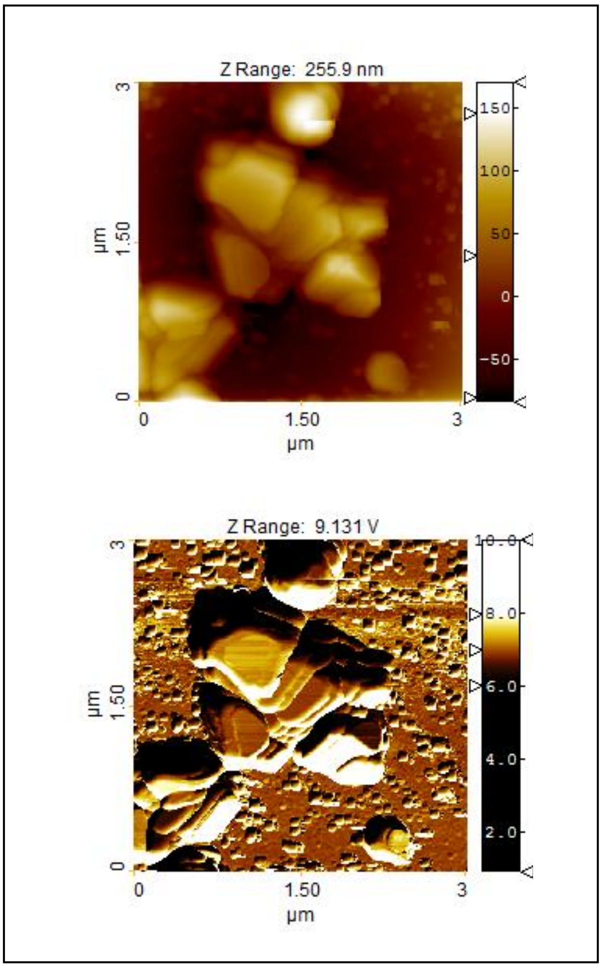

Figure 11. Topography (top) and the amplitude response of the force modulation mode (bottom) of investigated TiO_2-2-Ag-1 sample

The data analysis requires simultaneous observation both: the topography and FMM response images, as the topographical features such as the grains and the substrate should be correlated with the stiffness map. One can see, that the in general the grains reveal higher stiffness (brighter FMM response colors) than the substrate (darker colors), as it is expected concerning the fact, that the substrate is covered with the cured glue film. It should be underlined, that topographical features can have an impact on local FMM response, as the tip-sample contact area or angle can vary. Therefore the analysis was performed in flat and horizontally oriented areas.

To obtain TiO_2-Ag titania powder with the average grain size 170 nm was used as starting material, and the crystal phase was anatase (TiO_2-2). The synthesis of TiO_2-2-Ag-y (or ya) powders with various amount of silver (1, 5 and 10%) allows the formation of solids with such important properties as: (i) extended the $\lambda_{abs.}$ to higher wavelengths for the compounds with 5 and 10 % of silver (from about 330 to 620 nm), (ii) modified the topography of powders and (iii) changed the zeta potentials of titania. In the absence of Ag TiO_2-2 had negative zeta potentials changed along with change the pH from 4 to 10 (from -11 to -34 mV, respectively). For the doped with Ag titania nanomaterials also negative zeta potentials were found, however along with increase the amount of Ag and method of synthesis titania-silver powders some differences were found. In the presence of 1% of Ag, TiO_2-2-Ag-1 had negative zeta potentials less than -16 mV at pH 4, and greater than -28 mV at pH 10. Nanoparticles TiO_2-2 with 5% of Ag exhibited higher values of zeta potentials at pH 4 than TiO_2-2-Ag-1 (-19 mV). Similar behavior was found for the compounds TiO_2-2-Ag-ya (for pH 4: -14 mV, for ph: 10 -18 mV for TiO_2-2-Ag-1a, and for pH 4: -20 mV, for ph 10: -24 mV for TiO_2-2-Ag-5a). It indicates that the amount of Ag along with method of titania-silver synthesis influences on the properties of titania. Probably ions imparted negative charge to undoped nanoparticles TiO_2-2 surfaces and increased their absolute surface potentials. Additional work is necessary to confirm our suggestions.

4. Conclusions

In this work we presented the results of the investigation of the morphological and optical properties of the TiO_2 and Ag doped TiO_2 powder. Utilized techniques such as AFM, SEM, EDS, XRD and UV-vis allowed acquire essential information about developed materials. Both: AFM and SEM provided the diameter of the grains. Obtained values are coherent. Specific features of the grains, such as the shape related to the material's form, could be on the other hand observed using only AFM technique, which provides accurate 3D surface imaging. Such ability allowed verify that the anatase form was obtained, which was also detected with XPS. It was also shown, that the expected Ag content in grains was verified with EDS analysis. Additionally, the presence of silver spots on the surface of grains was detected using phase imaging technique. Utilization of the force modulation mode provided the information about the stiffness of the substrate and the material. It should be underlined however, that obtained data is qualitative; therefore no real value of the mechanical properties may be determined using this method. Performed UV-vis measurements allowed to learn that the increase of the silver content significantly reduces the light transmission for wavelength above 400 nm.

ACKNOWLEDGEMENTS

The authors thank dr J. Warycha for SEM and EDS measurements, dr. M. Palewicz for UV-vis measurements, Mss K. Gryzlo for zeta potential experiments and prof. W. Mielcarek for X-ray measurements.

INNOVATIVE ECONOMY
NATIONAL COHESION STRATEGY

EUROPEAN UNION
EUROPEAN REGIONAL DEVELOPMENT FUND

„The research was supported by Wroclaw Research Centre EIT+ under the project „The Application of Nanotechnology in Advanced Materials" – NanoMat (POIG.01.01.02-02-002/08) financed from the European Regional Development Fund (Operational Programme Innovative Economy, 1.1.2)"

REFERENCES

[1] Ananpattarachai J., Kajitvichyanukul P., Seraphin S., Visible light absorption ability and photocatalytic oxidation activity of various interstitial N-doped TiO_2 prepared from different nitrogen dopants, Journal of Hazardous Materials, 2009; 168, 253–261.

[2] Fujishima A., Hashimoto K., Watanabe T., TiO_2 Photocatalysis: Fundamentals and Applications, BKC Inc., Tokyo, 1999.

[3] Zhang Y., Chen Y., Westerhoff P., Crittenden J., Impact of natural organic matter and divalent cations on the stability of aqueous nanoparticles, Water Research, 2009; 43, 4249–4257.

[4] Ganesh I., Gupta A.K., Kumar P.P., Chandra Sekhar P.S., Radha K., Padmanabham G., Sundararajan G., Preparation and characterization of Co-doped TiO_2 materials for solar light induced current and photocatalytic applications, Materials Chemistry and Physics, 2012; 135, 220–234.

[5] Wang H-W., Lin H-C., Kuo C-H., Cheng Y-L., Yeh Y-C., The CMS experiment at the CERN LHC, Journal of Physics and Chemistry of Solids, 2008; 69, 633–636.

[6] Lai Y., Chen Y., Zhuang H., Lin C., The ATLAS Experiment at the CERN Large Hadron Collider, Materials Letters, 2008; 62, 3688–3690.

[7] Amin S.A., Pazouk M., Hosseinnia A., Synthesis of TiO_2–Ag nanocomposite with sol–gel method and investigation of its antibacterial activity against *E. coli*, Powder Technology, 2009; 196, 241-245.

[8] Li X.S., Fryxell G.E., Wang C., Engelhard M.H., The synthesis of Ag-doped mesoporous TiO_2, Microporous and Mesoporous Materials, 2008; 111, 639–642.

[9] Wua Q-H., Fortunellib A., Granozzi G., Preparation, characterisation and structure of Ti and Al ultrathin oxide films on metals, International Reviews in Physical Chemistry, 2009; 28, 517–576.

[10] Aysin B., Ozturk A., Park J., Silver-loaded TiO_2 powders prepared through mechanical ball milling, Ceramics International, 2013; 39, 7119–7126.

[11] Shi-Jie S., Li-Ping Y., Xiao-Min L., Xiao-Ling W., Hui Y., Xiao-Dong S., Preparation and characterization of TiO_2 doped and MgO stabilized Na-Al2O3 electrolyte via a citrate sol–gel method, Journal of Alloys and Compounds, 2013; 563, 176–179.

[12] Sriwong C., Wongnawa S., Patarapaiboolchai O., Photocatalytic activity of rubber sheet impregnated with TiO_2 particles and its recyclability, Catalysis Communications, 2012; 24(3) 464–472.

[13] Žunič V., Vukomanović M., Škapin S.D., Suvorov D., Kovač J., Photocatalytic properties of TiO_2 and TiO_2/Pt: A sol-precipitation, sonochemical and hydrothermal approach, Ultrasonics Sonochemistry (Article in press), DOI: 10.1016/j.ultsonch.2013.05.018.

[14] MacÉ T., Vaslin-Reimann S., Ausset P., Maillé M., Characterization of manufactured TiO_2 nanoparticles, Journal of Physics, 2013; 429, 012012 (10p).

[15] Niu J. Yao B. Chen Y., Peng C., Yu X., Zhang J., Bai G., Enhanced photocatalytic activity of nitrogen doped TiO_2 photocatalysts sensitized by metallo Co, Ni-porphyrins, Applied Surface Science, 2013; 271, 39-44.

[16] Sikora A., Woszczyna M., Friedemann M., Ahlers F.J., Kalbac M., AFM diagnostics of graphene-based quantum Hall devices, Micron, 2012; 43, 479-486.

[17] Lau J.W., Shaw J.M., Magnetic nanostructures for advanced technologies: fabrication, metrology and challenges. Journal of Physics D: Applied Physics, 2011; 44, 303001 (p43).

[18] Shi L., Plyasunov S., Bachtold A., McEuen P.L., Majumdar A.: Scanning thermal microscopy of carbon nanotubes using batch-fabricated probes, Applied Physics Letters, 2000; 77, 4295 (p3).

[19] Szymoński M., Goryl M., Krok F., Kolodziej J.J., Mongeot F.B.D, Metal nanostructures assembled at semiconductor surfaces studied with high resolution scanning probes, Nanotechnology, 2007; 18, 044016 (p7).

[20] Allers W., Schwarz A., Schwarz U.D., Wiesendanger R.: A scanning force microscope with atomic resolution in ultrahigh vacuum and at low temperatures, Review of Scientific Instruments, 1998; 69, 221-225.

[21] Jaafar M., Go J., Gómez-Herrero J., Gil a, Ares P., Vázquez M., Asenjo a: Variable-field magnetic force microscopy, Ultramicroscopy, 2009; 109, 693 (p9).

[22] Sikora A., Correction of structure width measurements performed with a combined shear-force/tunneling microscope, Measurement Science and Technology, 2007; 2, 456–461.

[23] Dongmo S., Vautrot P., Bonnet N., Troyon M., Correction of surface roughness measurements in SPM imaging, Applied Physics A, 1998; 66, 819–823.

[24] Matyka K., Matyka M., Mróz I., Zalewska-Rejdak J., Ciszewski A., An AFM study on mechanical properties of native and dimethyl suberimidate cross-linked pericardium tissue, Journal of molecular recognition, 2007; 20, 524–530.

[25] Ptak A., Makowski M., Cichomski M., Characterization of nanoscale adhesion between a fluoroalkyl silane monolayer and a silicon AFM tip. Complex character of the interaction potential, Chemical Physics Letters, 2010; 489, 54–58.

[26] Sikora A., Bednarz L., Mapping of mechanical properties of the surface by utilization of torsional oscillation of the cantilever in atomic force microscopy, Central European Journal of Physics, 2011; 9, 372–379.

[27] Magonov S.N.S., Elings V., Whangbo M.-H., Phase imaging and stiffness in tapping-mode atomic force microscopy, Surface Science, 1997; 375, L385–L391.

[28] Bar G., Brandsch R., Whangbo M.-H., Description of the frequency dependence of the amplitude and phase angle of a silicon cantilever tapping on a silicon substrate by the harmonic approximation, Surface Science, 1998; 411, L802–L809.

[29] Cleveland J.P., Anczykowski B., Schmid a. E., Elings V.B., Energy dissipation in tapping-mode atomic force microscopy, Applied Physics Letters, 1998; 72, 2613–2615.

[30] Anczykowski B., Gotsmann B., Fuchs H., Cleveland J.P., Elings V.B., How to measure energy dissipation in dynamic mode atomic force microscopy, Applied Surface Science, 1999; 140, 376–382.

[31] Sikora A., The method of minimizing the impact of local residual electrostatic charge on dimensional measurement accuracy in atomic force microscopy measurements, Measurement Science and Technology, 2011; 22, 94022 (p7).

[32] Chung J., Munz M., Sturm H., Stiffness variation in the interphase of amine-cured epoxy adjacent to copper microstructures, Surface and Interface Analysis, 2007; 39, 624-633.

[33] Radmacher M., Tillmann R.W., Gaub H.E., Imaging viscoelasticity by force modulation with the atomic force microscope, Biophysical Journal, 1992; 64, 735–742.

[34] Chuchmała A., Palewicz M., Sikora A., Iwan A., Influence of graphene oxide interlayer on PCE value of polymer solar cells, Synthetic Metals, 2013; 169, 33–40.

[35] Sikora A., Iwan A., AFM study of the mechanical wear phenomena of the polyazomethine with thiophene rings: Tapping mode, phase imaging mode and force spectroscopy, High Performance Polymers, 2012; 24, 218–228.

[36] Iwan A., Schab-Balcerzak E., Siwy M., Sikora A., Palewicz M., Janeczek H., Sibinski M., New aliphatic–aromatic tetraphenylphthalic-based diimides: Thermal, optical and electrical study, Optical Materials, 2011; 33, 958–967.

[37] Vijay M., Selvarajan V., Sreekumar K.P., Jiaguo Y., Shengwei L., Ananthapadmanabhan P.V., Characterization and visible light photocatalytic properties of nanocrystalline TiO_2 synthesized by reactive plasma processing, Solar Energy Materials & Solar Cells, 2009; 93, 1540–1549.

[38] Wen-Chi H., Yu-Chun C., Hsin C., Ting-Ke T., Synthesis and characterization of TiO_2 and Fe/TiO_2 nanoparticles and their performance for photocatalytic degradation of 1,2-dichloroethane, Applied Surface Science, 2008; 255, 2205–2213.

[39] Yanqin W., Humin C., Yanzhong H., Jiming M., Weihua L., Shengmin C., Preparation, characterization and photoelectrochemical behaviors of Fe(III)-doped TiO_2 nanoparticles, Journal of Materials Science, 1999; 34, 3721–3729.

[40] Yan J., Wang B., Hai-Ping C., Shi-Guo D., Low temperature preparetion and photo-absorbance property of micron sizw Cu/nano-TiO_2 composite particles, Journal of Inorganic Materials, 2010; 25, 370–374.

[41] Ishibai Y., Sato J., Nishikawa T., Miyagishi S., Synthesis of visible-light active TiO_2 photocatalyst with Pt-modification: Role of TiO_2 substrate for high photocatalytic activity, Applied Catalysis B: Environmental, 2008; 79, 117–121.